

## RESEARCH ARTICLE

# Microglia measured by TSPO PET are associated with Alzheimer's disease pathology and mediate key steps in a disease progression model

Samantha M. Rossano<sup>1</sup>  | Aubrey S. Johnson<sup>1</sup> | Anna Smith<sup>1</sup> | Galen Ziaggi<sup>1</sup> | Andrew Roetman<sup>1</sup> | Diana Guzman<sup>1</sup> | Amarachukwu Okafor<sup>1</sup> | Julia Klein<sup>2</sup> | Zeljko Tomljanovic<sup>1</sup> | Yaakov Stern<sup>1</sup> | Adam M. Brickman<sup>1</sup> | Seonjoo Lee<sup>3</sup> | William C. Kreisl<sup>1</sup> | Patrick Lao<sup>1</sup> 

<sup>1</sup>Department of Neurology, Taub Institute for Research on Alzheimer's Disease and the Aging Brain, Columbia University Irving Medical Center, New York, New York, USA

<sup>2</sup>Department of Anesthesiology and Perioperative Medicine, University of California Los Angeles Health, Los Angeles, California, USA

<sup>3</sup>Department of Psychiatry and Biostatistics, Columbia University Irving Medical Center, New York, New York, USA

## Correspondence

Patrick Lao, Department of Neurology, Taub Institute for Research on Alzheimer's Disease and the Aging Brain, Columbia University Irving Medical Center, New York, NY, USA. Email: [pjl2133@cumc.columbia.edu](mailto:pjl2133@cumc.columbia.edu)

## Funding information

National Institutes on Aging of the NIH, Grant/Award Numbers: K23AG052633, R01AG026158, R56AG034189, R00AG065506, P30AG66462, P01AG07232, R01AG037212, RF1AG054023

## Abstract

**INTRODUCTION:** Evidence suggests microglial activation precedes regional tau and neurodegeneration in Alzheimer's disease (AD). We characterized microglia with translocator protein (TSPO) positron emission tomography (PET) within an AD progression model where global amyloid beta (A $\beta$ ) precedes local tau and neurodegeneration, resulting in cognitive impairment.

**METHODS:** Florbetaben, PBR28, and MK-6240 PET, T1 magnetic resonance imaging, and cognitive measures were performed in 19 cognitively unimpaired older adults and 22 patients with mild cognitive impairment or mild AD to examine associations among microglia activation, A $\beta$ , tau, and cognition, adjusting for neurodegeneration. Mediation analyses evaluated the possible role of microglial activation along the AD progression model.

**RESULTS:** Higher PBR28 uptake was associated with higher A $\beta$ , higher tau, and lower MMSE score, independent of neurodegeneration. PBR28 mediated associations between tau in early and middle Braak stages, between tau and neurodegeneration, and between neurodegeneration and cognition.

**DISCUSSION:** Microglia are associated with AD pathology and cognition and may mediate relationships between subsequent steps in AD progression.

## KEYWORDS

AD progression, Alzheimer's disease, neuroinflammation, TSPO PET

## 1 | BACKGROUND

Diffuse amyloid  $\beta$  (A $\beta$ ) deposition throughout the neocortex<sup>1</sup> can occur as early as two decades before Alzheimer's disease (AD) symptom onset and is believed to facilitate the development of other AD

pathologies, including the aggregation of hyperphosphorylated tau into neurofibrillary tangles.<sup>2,3</sup> The spread of tau pathology in AD has been well characterized into Braak stages at autopsy,<sup>4</sup> starting with early accumulation in the entorhinal cortex and hippocampal regions before spreading to other regions of the temporal, frontal, and

This is an open access article under the terms of the [Creative Commons Attribution-NonCommercial-NoDerivs](https://creativecommons.org/licenses/by-nc-nd/4.0/) License, which permits use and distribution in any medium, provided the original work is properly cited, the use is non-commercial and no modifications or adaptations are made.

© 2024 The Authors. *Alzheimer's & Dementia* published by Wiley Periodicals LLC on behalf of Alzheimer's Association.

parietal regions. Of note, the spatiotemporal trajectory of tau aggregation precedes that of neurodegeneration (eg, neuronal death, synaptic loss), which gives rise to AD symptoms.<sup>5</sup> This model of A $\beta$  deposition to tau aggregation across Braak stages to neurodegeneration to cognitive impairment will be referred to as the AD progression model throughout this article.

Neuroinflammation is an immune response in which glial cells in the brain, such as microglia, are recruited to protect tissue from pathogens, respond to injury, and help with the upkeep of tissue maintenance. Microglia are heterogeneous in their developmental origins as well as their varied response to stimuli during surveillance, including the adoption of different cellular morphologies and differential transcriptomic expression through aging, injury, and disease, suggesting context-dependent functionality over time within a single microglia.<sup>6</sup> Within the context of AD, microglial activity plays a complex role, where it may protect against disease pathology, promote the spread of disease pathology, or be a product of disease progression. Microglia may serve a protective function, such as clearing soluble A $\beta$  or corralling larger A $\beta$  deposits in the extracellular space, maintaining an innate immune memory; however, primed microglia can develop a complex neurotoxic phenotype with exaggerated immune responses leading to chronic inflammation or an attenuated immune response leading to unchecked pathology, depending on the stimuli, the microenvironment, and the cellular cross-talk with neurons and other inflammatory cells.<sup>7,8</sup> These dysfunctional microglia are associated with increased A $\beta$  and AD risk.<sup>9</sup> Further, apolipoprotein E (APOE) and triggering receptor expressed on myeloid cells 2 (TREM2) mutations in microglia may promote amyloidosis and tauopathies through their role in leading to or suppressing microglial activation.<sup>10</sup> Microglial activation may also promote disease pathology and progression via cytokine release<sup>9</sup> and the NOD-, LRR-, and pyrin domain-containing protein 3 (NLRP3) inflammasome,<sup>2,11-17</sup> preceding<sup>13,14,18-20</sup> and seeding<sup>21-23</sup> tau pathology to surrounding unaffected areas as well as contributing to amyloid-initiated, tau-dependent synaptic loss.<sup>9,24</sup> Microglia, as a product of disease progression, can perform cellular functions related to the upkeep of the extracellular space (ie, removing cellular waste and debris).<sup>25</sup> The accumulation of insoluble myelin debris within surveilling microglia can ultimately lead to microglia dysfunction, brain aging,<sup>26</sup> and cognitive impairment.<sup>27</sup> The complex age- and disease stage-dependent role of microglia likely contributes to the mixed results obtained in clinical trials of non-steroidal anti-inflammatory drugs (NSAIDs) to prevent or delay AD.<sup>28-30</sup> For a review of microglia heterogeneity and nomenclature, see Healy et al.<sup>6</sup> and Paolicelli et al.<sup>8</sup>

Moving beyond study designs that only include canonical A $\beta$ , tau, and neurodegeneration biomarkers, recent advancements have made it possible to incorporate the role of neuroinflammatory markers throughout AD progression.<sup>31</sup> The 18 kDa translocator protein (TSPO) can be imaged in vivo using positron emission tomography (PET)<sup>32</sup>; an elevated signal from TSPO PET can indicate activated microglia and/or increased microglial density. Regional TSPO expression, induced by amyloid, propagates across Braak stages and may be a driver of tau aggregation and spread in patients with AD,<sup>33</sup> yet TSPO in activated microglia is also closely associated with neurodegeneration.<sup>34</sup> We

## RESEARCH IN CONTEXT

- 1. Systematic review:** The authors reviewed the literature using traditional sources (eg, PubMed) and cite these studies appropriately. The role of key proteins, including amyloid  $\beta$  (A $\beta$ ) and tau, has been well characterized in Alzheimer's disease (AD), while the mechanisms by which neuroinflammation is related to disease progression remain uncertain.
- 2. Interpretation:** This study shows that neuroinflammation is not only related to measures of AD such as A $\beta$  and tau burden but also may mediate important steps in the progression of disease pathology. These findings support the hypothesis that activated microglia contribute to the spread of AD pathology and, in turn, symptomology.
- 3. Future directions:** Future studies should explore this in a longitudinal manner by repeating measures in the same patient to explore within-subject AD progression. A better understanding of AD progression will contribute to improved treatments and cognitive outcomes for those with the disease.

sought to determine whether TSPO had both upstream (ie, preceding neurodegeneration) and downstream (ie, following neurodegeneration) associations with AD pathology. First, we examined the association of TSPO with measures of (1) global A $\beta$ , (2) regional tau across different Braak stages, and (3) cognition, while accounting for neurodegeneration. Next, we considered the role of TSPO in AD based on a progression model that began with A $\beta$  deposition and continues with tau aggregation and neurodegeneration in early, middle, and late Braak stages, followed by cognitive impairment.

## 2 | METHODS

### 2.1 | Participants

Forty-one research participants underwent magnetic resonance imaging (MRI), multiple PET scans, and a cognitive assessment. These participants were retrospectively selected from and harmonized across studies (K23AG052633, R01AG026158, R56AG034189, P50AG008702, P01AG07232, R01AG037212, RF1AG054023),<sup>35,36</sup> based on the availability of imaging and cognitive measures. Of these participants, 19 were cognitively unimpaired, while 22 were cognitively impaired based on having a primary memory complaint and meeting clinical criteria for either amnesic mild cognitive impairment (MCI, single- or multiple-domain)<sup>37</sup> or AD,<sup>38</sup> as described previously.<sup>36</sup> Participants were evaluated with the Mini-Mental State Examination (MMSE<sup>39</sup>), and domain-specific tests including the Selective Reminding Test-Delayed Recall (SRT-DR<sup>40</sup>), Trail Making Test Part B (Trails B<sup>41</sup>),

and categorical fluency (CF-Animals<sup>42</sup>). Domain-specific cognitive test scores were transformed into z-scores using age-, sex-, and education-adjusted normative data derived from the National Alzheimer's Coordinating Center Uniform Dataset (NACC).<sup>43</sup> All participants (or their legally authorized representatives) provided informed consent according to the Declaration of Helsinki, and all study procedures were approved by the Columbia University Irving Medical Center Institutional Review Board.

## 2.2 | TSPO genotyping

TSPO binding affinity was determined at screening, as previously described.<sup>36</sup> Briefly, genomic DNA from each subject was used to genotype the rs6971 polymorphism using a TaqMan assay.<sup>44</sup> Participants were high-affinity binders (HH) or mixed-affinity binders (HL), and the proportion did not differ between controls and patients. Low-affinity binders (LL) were excluded.

## 2.3 | APOE genotyping

APOE information was only available in a subset of 17 participants (10 controls, seven patients). All patients were APOE  $\epsilon$ 4 non-carriers, which precluded robust interpretation of models when including APOE  $\epsilon$ 4 status. However, APOE  $\epsilon$ 4 carriers had significantly greater global <sup>18</sup>F-florbetaben (FBB) SUVR and MK6240 SUVR and lower global cognition, with slightly greater PBR28 SUVR and lower %GM (Table S1).

## 2.4 | Magnetic resonance imaging

MRI scans were acquired as previously described.<sup>35,36</sup> In short, all participants underwent T1-weighted MRI scanning on a 3T scanner. FreeSurfer 6.0 (Massachusetts General Hospital, Harvard Medical School; <http://surfer.nmr.mgh.harvard.edu>) was used to segment the MRI scans and to determine gray matter (GM) volume. A global neurodegeneration measure (%GM) was calculated as the sum of the GM volume from composite AD-related regions (hippocampus, inferior frontal gyrus, middle-inferior and superior temporal cortex, medial temporal cortex, inferior and superior parietal cortex, precuneus, prefrontal cortex, and posterior cingulate) normalized by the total intracranial volume. Neurodegeneration measures were also calculated for early (I+II), middle (III+IV), and late (V+VI) Braak stages (Table S2). Divisions of Braak staging have been described elsewhere.<sup>35,45</sup>

## 2.5 | PET

### 2.5.1 | Image acquisition, processing, and quantification

#### <sup>18</sup>F-Florbetaben (FBB)

FBB scans were acquired to evaluate A $\beta$  as described previously.<sup>36</sup> In summary, image data from 50 to 70 min after FBB injection were

aligned with the MRI, and regions of interest (ROIs) were defined using the Hammers-N30R83-1 MM atlas in the PNEURO module of PMOD 3.9 (PMOD Technologies<sup>46</sup>). Amyloid positivity was defined as previously described.<sup>36</sup> Partial volume correction (PVC) was completed using the region-based voxel-wise method (PMOD Technologies<sup>47</sup>). Standardized uptake value ratios (SUVRs) were calculated by normalizing the radioactivity in the ROIs to the activity in the GM of the cerebellum. A composite SUVR measure was calculated based on a volume-weighted average of representative AD-related regions consisting of the same regions as mentioned earlier for the composite MRI measure.

#### <sup>11</sup>C-PBR28 (PBR28)

PBR28 scans were acquired to evaluate TSPO expression, as described previously.<sup>36</sup> In summary, image data from 60 to 90 min after PBR28 injection were aligned with the MRI, and ROIs were defined using the Hammers-N30R83-1 MM atlas in the PNEURO module of PMOD 3.9. PVC was completed using the region-based voxel-wise method in PMOD. SUVR measures were calculated by normalizing the radioactivity in the ROIs to the activity in the GM of the cerebellum, which was used as a reference region. A composite SUVR measure was calculated based on a volume-weighted average of representative AD-related regions consisting of the same regions as mentioned above for the composite FBB and MRI measures.

#### <sup>18</sup>F-MK-6240 (MK-6240)

MK-6240 scans were acquired to evaluate the presence and extent of tau pathology, as described previously.<sup>35</sup> In summary, image data were collected from 90 to 110 min after MK-6240 injection. ROIs were defined in FreeSurfer. Tau positivity thresholds for early, middle, and late Braak stages (individual regions outlined in Table S2) were 1.40, 1.50, and 1.53 SUVR, respectively, and were previously derived in a sample of 100 cognitively unimpaired adults from a community-based study in Northern Manhattan.<sup>35</sup> PVC was implemented in MATLAB using the Muller-Gartner method<sup>47</sup> as performed in the previous study.<sup>35</sup> SUVR measures were calculated using the inferior GM of the cerebellum as a reference region, which avoids spill-in of radio-tracer binding in the occipital lobe and off-target binding in the falx cerebelli. Regional SUVR measures were calculated for early (I+II), middle (III+IV), and late (V+VI) Braak stages, as described above for the regional MRI measures.

## 2.6 | Statistical analysis

Demographic characteristics between the control and patient groups were compared with t-tests for continuous variables and chi-squared tests for proportional variables for context related to AD progression, but data from both groups were combined for the association and mediation analyses. To test whether TSPO expression was associated with AD biomarkers and cognition independently of neurodegeneration, we used a series of linear regressions with PBR28 SUVR as the independent variable and AD biomarkers (FBB SUVR, MK-

6240 SUVR) or cognitive performance (MMSE, SRT-DR, Trails B, CF-Animals) as the dependent variable controlling for age, education, race, sex, and *TSPO* genotypes, with and without %GM in an AD composite region (Figure S1). To evaluate whether *TSPO* expression mediated pathways along the AD progression model, we performed a series of structural equation models (lavaan package, R version 4.1.2<sup>48</sup>; standard errors computed using Delta method<sup>49</sup>), adjusting each path for age, education, race, sex, and *TSPO* genotypes. For the AD progression model, regional %GM within early, middle, and late Braak stages was used rather than %GM in an AD composite region.

The main analyses were performed using PVC PET data to account for spill-out of PET signal due to neurodegeneration within a voxel; PVC methods may add noise to data,<sup>50</sup> and analyses using uncorrected PET data are shown in Figures S2 and S3 and Table S3. Some PET measures were skewed. While very high values in patients relative to controls are biologically plausible and meaningful, we repeated the analysis after log transformation. Reported results were not biased by the skewness of PET data. Corrections for multiple comparisons were not performed. All analyses were performed using R version 4.1.2.

### 3 | RESULTS

#### 3.1 | Demographic characteristics

Age did not differ between controls and patients, and there were more men, more White participants, and greater years of education in the patient group (Table 1). As expected, the patient group had greater FBB SUVR, greater PBR28 SUVR, greater MK-6240 SUVR in early, middle, and late Braak stages, and lower MMSE, SRT-DR, Trails B, and CF-Animals scores. Notably, the patient group had the greatest MK-6240 SUVR in middle Braak regions and the lowest SRT-DR scores, as expected, but the greatest impairment (ie, lowest individual-level z-scores) in Trails B.

#### 3.2 | *TSPO* correlates with AD PET and cognitive measures, independent of neurodegeneration

When correcting for %GM, greater PBR28 SUVR was associated with greater FBB SUVR (Figure 1;  $\beta = 0.46$ ,  $p = .002$ ). Greater PBR28 SUVR was also associated with greater MK-6240 SUVR in middle ( $\beta = 0.45$ ,  $p = .004$ ) and late ( $\beta = 0.50$ ,  $p = .002$ ) Braak regions, with a non-significant positive association in early Braak regions. Greater PBR28 SUVR was associated with lower MMSE ( $\beta = -0.53$ ,  $p = .006$ ), SRT-DR ( $\beta = -0.39$ ,  $p = .037$ ), and Trails B scores ( $\beta = -0.50$ ,  $p = .004$ ), but not categorical fluency scores. When not correcting for %GM, greater PBR28 SUVR was associated with greater MK-6240 SUVR in early Braak regions and lower CF-Animals score (Figure S1).

#### 3.3 | *TSPO* significantly mediates pathways along AD progression model

In a series of mediation analyses (Figure 2, Table 2), greater PBR28 SUVR mediated the association between greater MK-6240 SUVR in early Braak regions and greater MK-6240 SUVR in middle Braak regions (indirect effect = 0.118, z-score = 2.169,  $p = .030$ ) and the association between greater MK-6240 SUVR in middle Braak regions and greater neurodegeneration in middle Braak regions (indirect effect =  $-0.225$ , z-score =  $-2.214$ ,  $p = .027$ ). Greater PBR28 SUVR mediated the association between greater neurodegeneration in both early (indirect effect = 0.233, z-score = 2.307,  $p = .021$ ) and middle Braak regions (indirect effect = 0.204, z-score = 2.185,  $p = .029$ ) and lower MMSE score. Greater PBR28 SUVR also mediated the association between greater neurodegeneration in both early (indirect effect = 0.283, z-score = 2.579,  $p = .009$ ) and middle Braak regions (indirect effect = 0.228, z-score = 2.379,  $p = .017$ ) and lower Trails B score.

### 4 | DISCUSSION

We examined the associations of microglial recruitment and/or density, measured by *TSPO* expression, and key AD biomarkers and cognitive measures with two goals – to disentangle components of neuroinflammation that drive pathology from those that respond to neurodegenerative processes and to elucidate the role of neuroinflammation along an AD progression model. Our findings add to the growing body of evidence that neuroinflammation tracks in severity with A $\beta$  and tau pathology and cognition, independently of the microglial response to neurodegenerative processes. The findings additionally demonstrate that neuroinflammation may be the mechanistic link by which tau spreads across Braak regions and between tau burden, neurodegeneration, and cognitive impairment.<sup>51</sup> Neuroinflammation should be incorporated into large-scale, multimodal studies of AD to understand the role of activated microglia in the links between A $\beta$  and tau, tau burden across Braak stage regions, and tau and downstream neurodegeneration and cognitive impairment such that specific inflammatory processes can be targeted at specific points along the AD continuum.

We found that greater *TSPO* expression was associated with AD severity in terms of neuropsychological testing results, GM volumes, and both A $\beta$  and tau burden, aligning with previous studies.<sup>33,52–54</sup> However, previous studies did not correct for neurodegeneration, so whether microglia were driving AD pathogenesis or responding to neurodegeneration had not been previously established. The current study suggests that the relationships between *TSPO* expression, AD biomarkers, and cognition are present regardless of the role of microglia in removing cellular debris and other neurodegeneration-related products. While we did not have the statistical power to test associations within controls and patients separately, it should be noted that a range of *TSPO* expression was present at low levels of tau in controls (Figure 1), potentially suggesting that neuroinflammation

**TABLE 1** Descriptive statistics of demographic characteristics and primary outcomes.

		Control (N = 19)	Patient (N = 22)	All (N = 41)	p value
Age	Mean (SD)	70.0 (4.3)	68.1 (8.7)	69.0 (7.0)	.401
	Range	60 to 76	53 to 83	53 to 83	
Sex	Female	10 (53%)	5 (22%)	15 (37%)	.047
	Male	9 (47%)	17 (77%)	26 (63%)	
Race	Black/African-American	5 (26%)	0 (0%)	5 (12%)	.010
	White	14 (74%)	22 (100%)	36 (88%)	
Education	Mean (SD)	15.4 (2.7)	17.1 (2.4)	16.3 (2.7)	.033
	Range	10 to 20	12 to 20	10 to 20	
TSPO genotype	HH	13 (68%)	13 (59%)	26 (63%)	.536
	HL	6 (32%)	9 (41%)	15 (37%)	
APOE ε4 status	Non-carriers	8 (42%)	2 (9%)	10 (24%)	<.001
	Carriers	7 (37%)	0 (0%)	7 (17%)	
	Missing	4 (21%)	20 (91%)	24 (59%)	
Amyloid status	Negative	12 (63%)	8 (36%)	20 (49%)	.087
	Positive	7 (37%)	14 (64%)	21 (51%)	
Early tau status	Negative	10 (53%)	2 (9%)	12 (29%)	.002
	Positive	9 (47%)	20 (91%)	29 (71%)	
Middle tau status	Negative	13 (68%)	4 (18%)	17 (41%)	.001
	Positive	6 (32%)	18 (82%)	24 (59%)	
Late tau status	Negative	14 (74%)	6 (27%)	20 (49%)	.003
	Positive	5 (26%)	16 (73%)	21 (51%)	
Composite <sup>18</sup> F-FBB PVC SUVR	Mean (SD)	1.47 (0.33)	1.88 (0.46)	1.69 (0.45)	.003
	Range	1.12 to 2.17	1.11 to 2.81	1.11 to 2.81	
Composite <sup>11</sup> C-PBR28 PVC SUVR	Mean (SD)	1.10 (0.11)	1.21 (0.10)	1.16 (0.12)	.001
	Range	0.77 to 1.22	1.06 to 1.45	0.77 to 1.45	
Early Braak <sup>18</sup> F-MK-6240 PVC SUVR	Mean (SD)	1.50 (0.51)	2.46 (0.91)	2.02 (0.886)	<.001
	Range	0.97 to 2.91	1.00 to 3.82	0.97 to 3.82	
Middle Braak <sup>18</sup> F-MK-6240 PVC SUVR	Mean (SD)	1.41 (0.21)	2.85 (1.54)	2.18 (1.34)	<.001
	Range	1.11 to 1.90	1.02 to 5.79	1.02 to 5.79	
Late Braak <sup>18</sup> F-MK-6240 PVC SUVR	Mean (SD)	1.39 (0.19)	2.55 (1.41)	2.01 (1.18)	<.001
	Range	1.09 to 1.75	0.98 to 5.99	0.98 to 5.99	
%GM volume	Mean (SD)	0.44 (0.01)	0.43 (0.01)	0.44 (0.01)	.017
	Range	0.43 to 0.46	0.39 to 0.45	0.39 to 0.46	
MMSE	Mean (SD)	29.2 (1.31)	25.6 (3.20)	27.3 (3.07)	<.001
	Range	26 to 30	18 to 30	18 to 30	
SRT-DR z-score	Mean (SD)	0.53 (1.09)	-3.11 (0.66)	-1.42 (2.04)	<.001
	Range	-1.60 to 2.27	-3.87 to 1.53	-3.87 to 2.27	
Trails B z-score	Mean (SD)	0.15 (0.64)	-2.79 (2.57)	-1.43 (2.42)	<.001
	Range	-1.23 to 1.02	-6.28 to 0.42	-6.26 to 1.02	
CF-Animals z-score	Mean (SD)	-0.24 (0.88)	-1.65 (1.17)	-0.98 (1.25)	<.001
	Range	-2.06 to 1.26	-3.31 to 2.38	-3.31 to 2.38	

Abbreviations: CF, categorical fluency; MMSE, Mini-Mental State Examination; SRT-DR, Selective Reminding Test-Delayed Recall; SUVR, standardized uptake value ratio; TSPO, translocator protein.



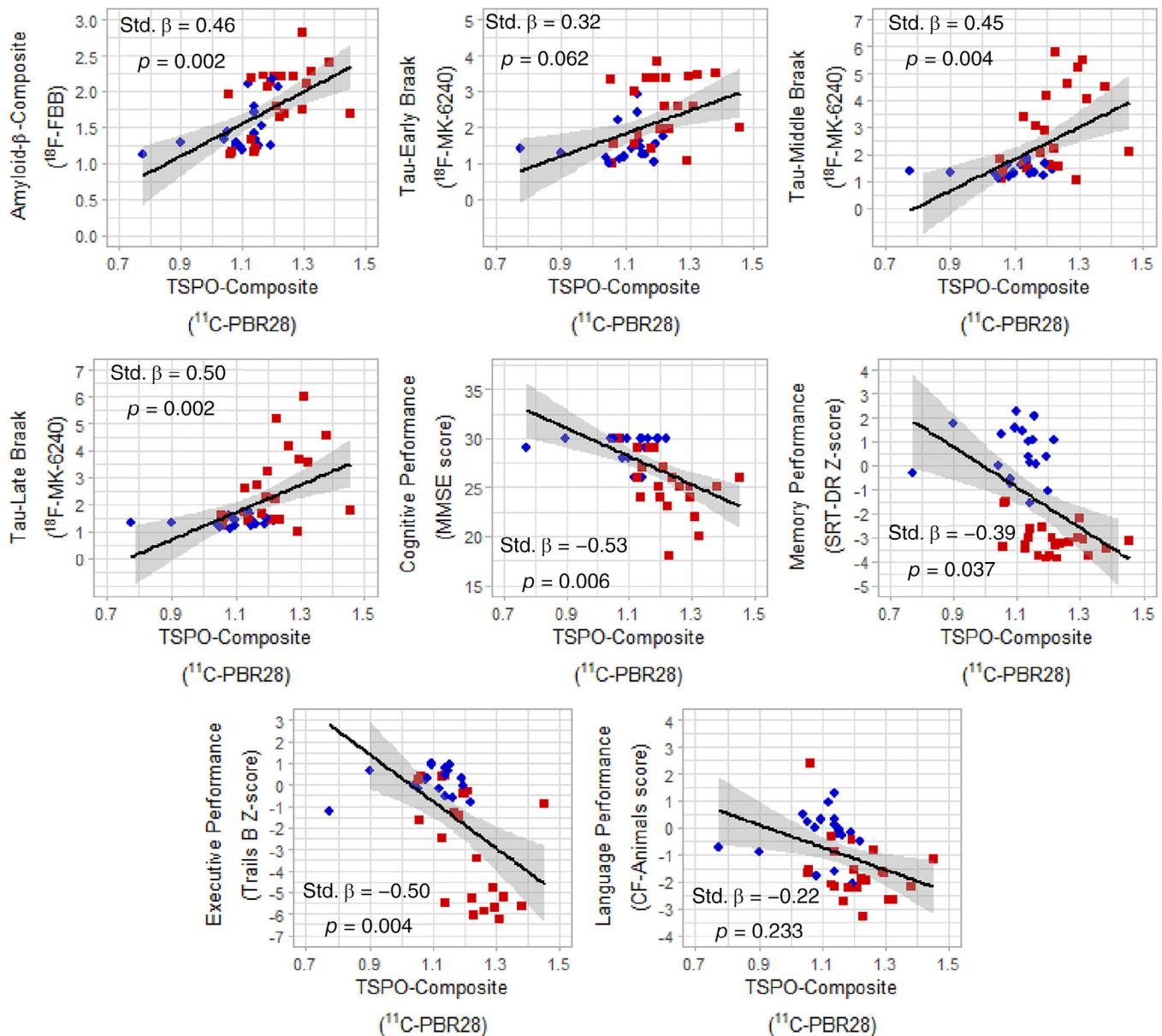


**FIGURE 1** TSPO expression by  $^{11}\text{C}$ -PBR28 uptake (SUVR) correlated with AD-related PET and cognitive measures across controls (blue circles) and patients (red squares). All associations were corrected for age, sex, race, education, TSPO genotype, and neurodegeneration (%GM in AD composite region). PET, positron emission tomography; SUVR, standardized uptake value ratio; TSPO, translocator protein.

precedes tau accumulation. Within patients, greater tau burden was observed in the presence of greater TSPO expression across Braak stage regions, and the association across controls and patients was independent of neurodegenerative processes in middle and late Braak stage regions. The association between greater TSPO expression and greater tau burden in early Braak stage regions did not survive adjustment for neurodegeneration. As tau spreads from across Braak stage regions, tau continues to increase in early Braak stage regions; tau burden in early Braak stage regions across controls and patients may reflect disease progression in a similar way to neurodegeneration. Therefore, there may be a mechanistic link between TSPO and tau in early Braak stage regions, but it may be too collinear with neurodegeneration across the clinical AD continuum to be identified using

cross-sectional data. Further work investigating regional TSPO, AD biomarkers, neurodegeneration, and cognition at distinct stages of the AD continuum is needed (eg, using amyloid-positive controls to test associations in early Braak stage regions).

We found that TSPO expression mediated the association between tau in early and middle Braak stage regions, between tau and neurodegeneration in middle Braak stages, and between neurodegeneration and cognitive impairment in early and middle Braak stages. To our knowledge, this is the first study to examine this type of TSPO mediation in an AD progression model from  $\text{A}\beta$  through tau, neurodegeneration, and cognition. Our results do not show a mediation effect of TSPO on the relationships between  $\text{A}\beta$  and tau in early Braak stages, between tau in early Braak stages and neurodegeneration, or

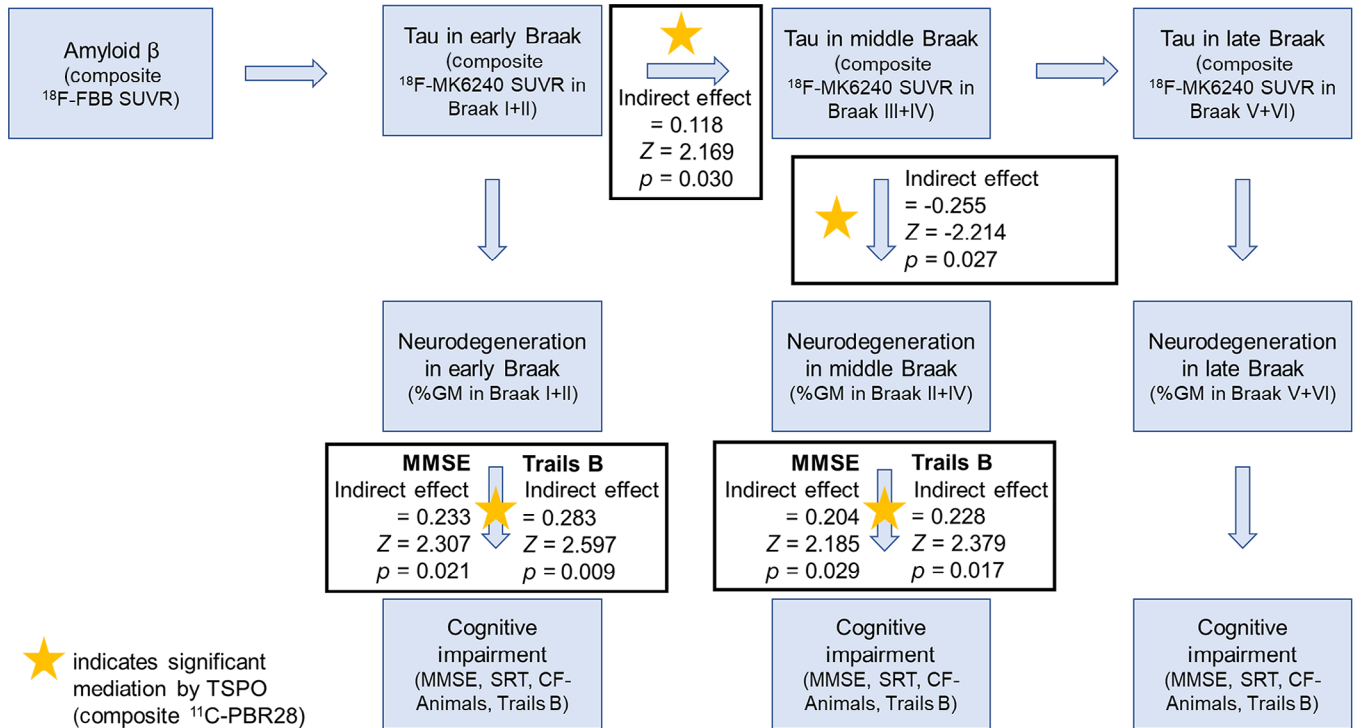


**FIGURE 2** TSPO expression by  $^{11}\text{C-PBR28}$  uptake (SUVR) significantly mediated pathways along AD progression model. SUVR, standardized uptake value ratios; TSPO, translocator protein.

throughout any steps in the late Braak pathway. Patients had the greatest tau burden in middle Braak stage regions and the greatest range of impairment in Trails B; it may be the case that the current sample did not have advanced enough tau pathology in late Braak stage regions to elucidate the roles of tau and neurodegeneration in late Braak stage regions but advanced enough tau pathology for measures in early Braak stages to have plateaued. Regardless, these analyses are an important step toward characterizing neuroinflammation in AD progression.

The findings of this study are in agreement with the extant literature and current research frameworks of AD, for example, AT(N)<sup>2,3</sup> and ATX(N)<sup>31</sup>, which were the basis of the longitudinal AD progression model investigated here. Our well-characterized sample with and without clinical impairment leveraged multiple studies and centers to perform broad neuroimaging characterization of TSPO PET in AD progression. Given that the results represented here are a secondary analysis of previously published data, PET methods (ROI definitions and PVC methods) for tau were defined differently than those of A $\beta$  and TSPO; however, consistency within radioligands is more important than consistency across radioligands for each participant, particularly as each method has been shown to reliably quantify the underlying pathology.<sup>55-57</sup> In the current sample, approximately 35% of patients were amyloid-negative. This aligns with previous reports of the mismatch between clinical AD and *post mortem* histopathological confirmation.<sup>58</sup> Participants who were amyloid-negative but tau-positive were similar to amyloid-positive and tau-positive participants

in terms of age, cortical thickness, memory-biomarker associations, and more.<sup>59</sup>

The study's limitations include its small sample size, lack of APOE information, and TSPO PET as a general marker. The inclusion of only a few participants in the early stages of AD pathogenesis, that is, cognitively normal but amyloid-positive and tau-negative, may limit our ability to detect early effects (eg, TSPO-mediating amyloid to tau associations). Therefore, our results may be capturing a microglial pathway specific to tau (eg, TSPO-mediated tau spreading and downstream neurodegeneration and cognitive impairment) that is simply apparent in this range of the AD continuum. Alternatively, there may be a specific microglial response to tau that differs from that to amyloid,<sup>60</sup> and the pathway from amyloid to tau may depend on other aspects of neuroinflammation, including astrocyte reactivity, in cognitively normal, amyloid-positive individuals.<sup>61</sup> APOE  $\epsilon 4$  plays a modulatory role in neuroinflammation, such that APOE  $\epsilon 4$  attenuates<sup>62</sup> or exaggerates<sup>63</sup> microglial activation, but the missingness pattern of APOE information precludes its inclusion in models. Simple main effects demonstrated higher PBR28 SUVR in APOE  $\epsilon 4$  carriers, in addition to its known effects on amyloid, tau, neurodegeneration, and cognition. While TSPO is upregulated in microglial activation in rodent models, TSPO is not upregulated in humans due to a species-specific promoter region on the TSPO gene.<sup>64</sup> Further, TSPO is expressed mostly in microglia<sup>65</sup> but to a lesser extent in astrocytes and endothelial cells.<sup>64,66,67</sup> However, changes in TSPO PET signal have been reported across many different neurodegenerative diseases,<sup>68</sup> and the majority of TSPO

**TABLE 2** Results of mediation analyses for composite <sup>11</sup>C-PBR28 SUVR in AD progression model.

X	Mediator	Y	Indirect effect (std. $\beta$ , z, p)	Direct effect (std. $\beta$ , z, p)	Total effect (std. $\beta$ , z, p)
Global A $\beta$ burden	Global TSPO expression	Tau in early Braak	0.017, 0.195, .845	0.748, 5.259, .000	0.765, 6.895, 0.000
Tau in early Braak		Neurodegeneration in early Braak	-0.157, -1.917, .055	-0.229, -1.591, .112	-0.386, -2.870, 0.004
Neurodegeneration in early Braak		Cognitive impairment - MMSE	0.233, 2.307, .021	0.207, 1.310, .190	0.440, 2.821, 0.005
		Cognitive impairment - SRT-DR	0.117, 1.536, .125	0.492, 3.368, .001	0.609, 4.553, 0.000
	Cognitive impairment - CF-Animals	0.076, 0.982, .326	0.391, 2.456, .014	0.468, 3.276, 0.001	
Cognitive impairment - Trails B	Cognitive impairment - Trails B	0.283, 2.597, .009	-0.057, -0.384, .701	0.226, 1.443, .149	
	Tau in early Braak	Tau in middle Braak	0.118, 2.169, .030	0.634, 7.078, .000	0.752, 8.750, .000
	Tau in middle Braak	Neurodegeneration in middle Braak	-0.255, -2.214, .027	-0.087, -0.506, .613	-0.342, -2.295, .022
Neurodegeneration in middle Braak	Cognitive impairment - MMSE	0.204, 2.185, .029	0.347, 2.277, .023	0.552, 3.768, .000	
	Cognitive impairment - SRT-DR	0.158, 1.794, .073	0.310, 1.959, .050	0.469, 3.198, .001	
	Cognitive impairment - CF-Animals	0.061, 0.804, .422	0.454, 2.909, .004	0.515, 3.727, .000	
	Cognitive impairment - Trails B	0.228, 2.379, .017	0.211, 1.439, .150	0.439, 3.037, .002	
Tau in middle Braak	Tau in late Braak	0.029, 0.956, .335	0.917, 18.22, .000	0.947, 23.03, .000	
Tau in late Braak	Neurodegeneration in late Braak	-0.168, -1.382, .167	0.015, 0.077, .938	-0.153, -0.966, .334	
Neurodegeneration in late Braak	Cognitive impairment - MMSE	0.0146, 1.588, .112	0.157, 1.074, .283	0.303, 1.850, .064	
	Cognitive impairment - SRT-DR	0.114, 1.497, .134	0.191, 1.283, .200	0.305, 1.933, .053	
	Cognitive impairment - CF-animals	0.071, 1.251, .211	0.297, 1.983, .047	0.368, 2.450, .014	
	Cognitive impairment - Trails B	0.144, 1.603, .109	0.136, 1.003, .316	0.280, 1.180, .070	

Note: Rows of significant mediations are shown in bold.

Abbreviations: CF, categorical fluency; MMSE, Mini-Mental State Examination; SRT-DR, Selective Reminding Test-Delayed Recall; std, standardized; SUVR, standardized uptake value ratio; TSPO, translocator protein.

PET signals<sup>69,70</sup> likely reflect microglial recruitment and/or density rather than an explicit microglial activation process. Whether microglia are maintaining their homeostatic state, responding properly to a given stimulus in a given circumstance, or responding improperly to a given stimulus in a given circumstance is unknown with TSPO PET. Regardless, we have identified tau spreading and tau-related neurodegeneration and cognitive impairment as a critical time point to further investigate with cell type- and function-specific methods such as glycogen synthase kinase 3 (GSK-3), cyclooxygenase-1 (COX-1), or COX-2<sup>71</sup> in larger longitudinal studies.

Neuroinflammatory processes have been implicated in late-onset AD,<sup>72,73</sup> early-onset AD,<sup>74,75</sup> autosomal-dominant AD,<sup>76</sup> and AD in adults with Down syndrome.<sup>77</sup> In our work, neuroinflammation may play a critical role in tau spreading across Braak stages as well as

downstream neurodegenerative and cognitive consequences of tau burden, independently of neuroinflammatory processes that clear neurodegeneration-related products. Other studies have also suggested that elevated TSPO signal precedes tau deposition throughout Braak staging.<sup>33</sup> Specific pathways in the AD progression model (eg, tau burden in early and middle Braak stages) may be more or less relevant depending on disease stage and severity of the study sample, and further work should elucidate the specific neuroinflammatory processes and microglial activation states on which to intervene.<sup>10,78</sup> Disease-modifying drugs, particularly the recent U.S. Food and Drug Administration-approved A $\beta$ -targeting antibodies, aducanumab<sup>79,80</sup> and lecanemab,<sup>81,82</sup> need to be better characterized in relation to the inflammatory responses that are induced to clear A $\beta$  oligomers and protofibrils. Monitoring and controlling the inflammatory response



may lead to a reduction in amyloid-related imaging abnormalities (ARIA).<sup>83</sup> As other therapeutics are developed in clinical trials, treatment response stratification will be critical. One potential way to perform such stratification might be based on patterns of neuroinflammation that may precede distinct subtypes of tau burden<sup>84,85</sup> and neurodegeneration,<sup>86,87</sup> which have differential rates of cognitive decline.<sup>88</sup> Overall, neuroinflammation may be the mechanism by which tau spreads across Braak stage regions and leads to downstream neurodegeneration and cognitive impairments. TSPO PET using either <sup>11</sup>C-PBR28 or third-generation TSPO radioligands, such as <sup>11</sup>C-ER17671, offers a suitable method of identifying key regionally and temporally specific neuroinflammatory processes in AD and related dementias.

## ACKNOWLEDGMENTS

This study utilized data acquired from research supported by National Institutes of Health (NIH) grants: K23AG052633, R01AG026158, R56AG034189. Research reported in this publication was supported by the National Institute on Aging of the NIH under Award P30AG066462 (Columbia University Alzheimer's Disease Research Center). The content is solely the responsibility of the authors and does not necessarily represent the official views of the NIH. This study was additionally supported by the Washington Heights-Inwood Columbia Aging Project (WHICAP, P01AG07232, R01AG037212, RF1AG054023), and R00AG065506. <sup>18</sup>F-Florbetaben was supplied by Life Molecular Imaging. <sup>18</sup>F-MK-6240 was supplied by Cerveau Technologies. The authors acknowledge Dr. Regina Santella, who performed the TSPO genotyping work.

## CONFLICT OF INTEREST STATEMENT

WCK has a consulting agreement with Cerveau Technologies. However, Cerveau was not involved in the study design or interpretation of these results. No authors have conflicts of interest to report. Author disclosures are available in the [Supporting Information](#).

## CONSENT STATEMENT

All human subjects provided informed consent.

## ORCID

Samantha M. Rossano  <https://orcid.org/0000-0003-0986-9100>

Patrick Lao  <https://orcid.org/0000-0003-2243-3547>

## REFERENCES

1. Thal DR, Rub U, Orantes M, Braak H. Phases of A beta-deposition in the human brain and its relevance for the development of AD. *Neurology*. 2002;58:1791-1800.
2. Jack Jr. CR, Knopman DS, Jagust WJ, et al. Tracking pathophysiological processes in Alzheimer's disease: an updated hypothetical model of dynamic biomarkers. *Lancet Neurol*. 2013;12:207-216.
3. Jack Jr. CR, Bennett DA, Blennow K, et al. NIA-AA research framework: toward a biological definition of Alzheimer's disease. *Alzheimers Dement*. 2018;14:535-562.
4. Braak H, Braak E. Evolution of the neuropathology of Alzheimer's disease. *Acta Neurol Scand Suppl*. 1996;165:3-12.
5. Bejanin A, Schonhaut DR, La Joie R, et al. Tau pathology and neurodegeneration contribute to cognitive impairment in Alzheimer's disease. *Brain*. 2017;140(12):3286-3300.
6. Healy LM, Zia S, Plemel JRJCB. Towards a definition of microglia heterogeneity. *Commun Biol*. 2022;5:1114.
7. Li X, Li Y, Jin Y, et al. Transcriptional and epigenetic decoding of the microglial aging process. *Nature Aging*. 2023;1:24.
8. Paolicelli RC, Sierra A, Stevens B, et al. Microglia states and nomenclature: a field at its crossroads. *Neuron*. 2022;110:3458-3483.
9. Hansen DV, Hanson JE, Sheng Morgan. Microglia in Alzheimer's disease. *J Cell Biol*. 2018;217:459-472.
10. Krasemann S, Madore C, Cialic R, et al. The TREM2-APOE pathway drives the transcriptional phenotype of dysfunctional microglia in neurodegenerative diseases. *Immunity*. 2017;47:566-581.
11. Dani M, Wood M, Mizoguchi R, et al. Microglial activation correlates in vivo with both tau and amyloid in Alzheimer's disease. *Brain*. 2018;141:2740-2754.
12. Hanslik KL, Ulland TK. The role of microglia and the Nlrp3 inflammasome in Alzheimer's disease. *Front Neurol*. 2020;11:570711.
13. Hopp SC, Lin Y, Oakley D, et al. The role of microglia in processing and spreading of bioactive tau seeds in Alzheimer's disease. *J Neuroinflammation*. 2018;15:269.
14. Ising C, Venegas C, Zhang S, et al. NLRP3 inflammasome activation drives tau pathology. *Nature*. 2019;575:669-673.
15. Lee M, McGeer E, McGeer PL. Activated human microglia stimulate neuroblastoma cells to upregulate production of beta amyloid protein and tau: implications for Alzheimer's disease pathogenesis. *Neurobiol Aging*. 2015;36:42-52.
16. Stancu I-C, Cremers N, Vanrusselt H, et al. Aggregated Tau activates NLRP3-ASC inflammasome exacerbating exogenously seeded and non-exogenously seeded Tau pathology in vivo. *Acta Neuropathol*. 2019;137:599-617.
17. Venegas C, Kumar S, Franklin BS, et al. Microglia-derived ASC specks cross-seed amyloid- $\beta$  in Alzheimer's disease. *Nature*. 2017;552:355-361.
18. Eikelenboom P, Van Exel E, Hoozemans JJ, Veerhuis R, Rozemuller AJ, Van Gool WA. Neuroinflammation—an early event in both the history and pathogenesis of Alzheimer's disease. *Neurodegener Dis*. 2010;7:38-41.
19. Serrano-Pozo A, Mielke ML, Gómez-Isla T, et al. Reactive glia not only associates with plaques but also parallels tangles in Alzheimer's disease. *Am J Pathol*. 2011;179:1373-1384.
20. Sheffield LG, Marquis JG, Berman NE. Regional distribution of cortical microglia parallels that of neurofibrillary tangles in Alzheimer's disease. *Neurosci Lett*. 2000;285:165-168.
21. DeVos SL, Miller RL, Schoch KM, et al. Tau reduction prevents neuronal loss and reverses pathological tau deposition and seeding in mice with tauopathy. *Sci Transl Med*. 2017;9:eaag0481.
22. Takeda S, Commins C, DeVos SL, et al. Seed-competent high-molecular-weight tau species accumulates in the cerebrospinal fluid of Alzheimer's disease mouse model and human patients. *Ann Neurol*. 2016;80:355-367.
23. Walsh DM, Selkoe DJ. A critical appraisal of the pathogenic protein spread hypothesis of neurodegeneration. *Nat Rev Neurosci*. 2016;17:251-260.
24. Rajendran L, Paolicelli RC. Microglia-mediated synapse loss in Alzheimer's disease. *J Neurosci*. 2018;38:2911-2919.
25. Kettenmann H, Hanisch UK, Noda M, Verkhratsky A. Physiology of microglia. *Physiol Rev*. 2011;91:461-553.
26. Santos EN, Fields RD. Regulation of myelination by microglia. *Sci Adv*. 2021;7:eabk1131.
27. Wang F, Ren S-Y, Chen JF, et al. Myelin degeneration and diminished myelin renewal contribute to age-related deficits in memory. *Nat Neurosci*. 2020;23:481-486.

28. Hoozemans JJM, Veerhuis R, Rozemuller JM, Eikelenboom PJC, Targets ND-D. Soothing the inflamed brain: effect of non-steroidal anti-inflammatory drugs on Alzheimer's disease pathology. *CNS Neurol Disord Drug Targets*. 2011;10:57-67.
29. Arvanitakis Z, Grodstein F, Bienias J, et al. Relation of NSAIDs to incident AD, change in cognitive function, and AD pathology. *Neurology*. 2008;70:2219-2225.
30. In'T Veld BA, Ruitenbergh A, Hofman A, et al. Nonsteroidal anti-inflammatory drugs and the risk of Alzheimer's disease. *N Engl J Med*. 2001;345:1515-1521.
31. Hampel H, Cummings J, Blennow K, Gao P, Jack Jr. CR, Vergallo A. Developing the ATX(N) classification for use across the Alzheimer disease continuum. *Nat Rev Neurol*. 2021;17(9):580-589.
32. Kreisl WC, Fujita M, Fujimura Y, et al. Comparison of [11C]-(R)-PK 11195 and [11C] PBR28, two radioligands for translocator protein (18 kDa) in human and monkey: implications for positron emission tomographic imaging of this inflammation biomarker. *Neuroimage*. 2010;49:2924-2932.
33. Pascoal TA, Benedet AL, Ashton NJ, et al. Microglial activation and tau propagate jointly across Braak stages. *Nat Med*. 2021;27:1592-1599.
34. Kreisl WC, Lyoo CH, Liow JS, et al. Distinct patterns of increased translocator protein in posterior cortical atrophy and amnesic Alzheimer's disease. *Neurobiol Aging*. 2017;51:132-140.
35. Kreisl WC, Lao PJ, Johnson A, et al. Patterns of tau pathology identified with <sup>18</sup>F-MK-6240 PET imaging. *Alzheimers Dement*. 2022;18(2):272-282.
36. Zou J, Tao S, Johnson A, et al. Microglial activation, but not tau pathology, is independently associated with amyloid positivity and memory impairment. *Neurobiol Aging*. 2020;85:11-21.
37. Albert MS, DeKosky ST, Dickson D, et al. The diagnosis of mild cognitive impairment due to Alzheimer's disease: recommendations from the National Institute on Aging-Alzheimer's Association workgroups on diagnostic guidelines for Alzheimer's disease. *Alzheimers Dement*. 2011;7:270-279.
38. McKhann GM, Knopman DS, Chertkow H, et al. The diagnosis of dementia due to Alzheimer's disease: recommendations from the National Institute on Aging-Alzheimer's Association workgroups on diagnostic guidelines for Alzheimer's disease. *Alzheimers Dement*. 2011;7:263-269.
39. Folstein MF, Robins LN, Helzer JE. The mini-mental state examination. *Arch Gen Psychiatry*. 1983;40:812.
40. Ruff RM, Light RH, Quayhagen MJ. Selective reminding tests: a normative study of verbal learning in adults. *J Clin Exp Neuropsychol*. 1989;11:539-550.
41. Tombaugh TN. Trail making test A and B: normative data stratified by age and education. *Neuropsychol*. 2004;19:203-214.
42. Rosen WG. Verbal fluency in aging and dementia. *J Clin Neurophysiol*. 1980;2:135-146.
43. Shirk SD, Mitchell MB, Shaughnessy LW, et al. A web-based normative calculator for the uniform data set (UDS) neuropsychological test battery. *Alzheimers Res Ther*. 2011;3:32.
44. Owen DR, Yeo AJ, Gunn RN, et al. An 18-kDa translocator protein (TSPO) polymorphism explains differences in binding affinity of the PET radioligand PBR28. *J Cereb Blood Flow Metab*. 2012;32:1-5.
45. Pascoal TA, Benedet AL, Ashton NJ, et al. Publisher correction: microglial activation and tau propagate jointly across Braak stages. *Nat Med*. 2021;27:2048-2049.
46. Hammers A, Allom R, Koeppe MJ, et al. Three-dimensional maximum probability atlas of the human brain, with particular reference to the temporal lobe. *Hum Brain Mapp*. 2003;19:224-247.
47. Thomas BA, Erlandsson K, Modat M, et al. The importance of appropriate partial volume correction for PET quantification in Alzheimer's disease. *Eur J Nucl Med Mol Imaging*. 2011;38:1104-1119.
48. Rosseel YJ. Lavaan: an R package for structural equation modeling. *J Stat Softw*. 2012;48:1-36.
49. Sobel ME. Asymptotic confidence intervals for indirect effects in structural equation models. *Sociol Methodol*. 1982;13:290-312.
50. Yang J, Hu C, Guo N, Dutta J, et al. Partial volume correction for PET quantification and its impact on brain network in Alzheimer's disease. *Sci Rep*. 2017;7:13035.
51. Leng F, Edison P. Neuroinflammation and microglial activation in Alzheimer disease: where do we go from here? *Nat Rev Neurol*. 2021;17:157-172.
52. Kreisl WC, Lyoo CH, McGwier M, et al. In vivo radioligand binding to translocator protein correlates with severity of Alzheimer's disease. *Brain*. 2013;136:2228-2238.
53. Klein J, Yan X, Johnson A, et al. Olfactory impairment is related to tau pathology and neuroinflammation in Alzheimer's disease. *J Alzheimers Dis*. 2021;80:1051-1065.
54. Bradburn S, Murgatroyd C, Ray NJ. Neuroinflammation in mild cognitive impairment and Alzheimer's disease: a meta-analysis. *Ageing Res Rev*. 2019;50:1-8.
55. Barthel H, Gertz H-J, Dresel S, et al. Cerebral amyloid- $\beta$  PET with florbetaben (18F) in patients with Alzheimer's disease and healthy controls: a multicentre phase 2 diagnostic study. *Lancet Neurol*. 2011;10:424-435.
56. Betthausen TJ, Cody KA, Zammit MD, et al. In vivo characterization and quantification of neurofibrillary tau PET radioligand <sup>18</sup>F-MK-6240 in humans from Alzheimer disease dementia to young controls. *J Nucl Med*. 2019;60:93-99.
57. Lyoo CH, Ikawa M, Liow J-S, et al. Cerebellum can serve as a pseudo-reference region in Alzheimer disease to detect neuroinflammation measured with PET radioligand binding to translocator protein. *J Nucl Med*. 2015;56:701-706.
58. Beach TG, Monsell SE, Phillips LE, Kukull W. Accuracy of the clinical diagnosis of Alzheimer disease at National Institute on Aging Alzheimer Disease Centers, 2005-2010. *J Neuropathol Exp Neurol*. 2012;71:266-273.
59. Weigand AJ, Edwards LE, Thomas KR, Bangen KJ, Bondi MW. Comprehensive characterization of elevated tau PET signal in the absence of amyloid-beta. *Brain Commun*. 2022;4:fcac272.
60. Navarro V, Sanchez-Mejias E, Jimenez S, et al. Microglia in Alzheimer's disease: activated, dysfunctional or degenerative. *Front Aging Neurosci*. 2018;10:140.
61. Bellaver B, Povala G, Ferreira PC, et al. Astrocyte reactivity influences amyloid- $\beta$  effects on tau pathology in preclinical Alzheimer's disease. *Nat Med*. 2023;29(7):1775-1781.
62. Yin Z, Rosenzweig N, Kleemann KL, et al. APOE4 impairs the microglial response in Alzheimer's disease by inducing TGF $\beta$ -mediated checkpoints. *Nat Immunol*. 2023;24(11):1839-1853.
63. Ferrari-Souza JP, Lussier FZ, Leffa DT, et al. APOE  $\epsilon$ 4 associates with microglial activation independently of A $\beta$  plaques and tau tangles. *Sci Adv*. 2023;9:eade1474.
64. Nutma E, Fancy N, Weinert M, et al. Translocator protein is a marker of activated microglia in rodent models but not human neurodegenerative diseases. *Nat Commun*. 2023;14:5247.
65. Venneti S, Wang G, Nguyen J, Wiley CA, Neurology E. The positron emission tomography ligand DAA1106 binds with high affinity to activated microglia in human neurological disorders. *J Neuropathol Exp Neurol*. 2008;67:1001-1010.
66. Masdeu JC, Pascual B, Fujita MJ. Imaging neuroinflammation in neurodegenerative disorders. *J Nucl Med*. 2022;63:455-525.
67. Nutma E, Gebro E, Marzin MC, et al. Activated microglia do not increase 18 kDa translocator protein (TSPO) expression in the multiple sclerosis brain. *Glia*. 2021;69:2447-2458.
68. Gouilly D, Saint-Aubert L, Ribeiro MJ, et al. Neuroinflammation PET imaging of the translocator protein (TSPO) in Alzheimer's disease: an update. *Eur J Neurosci*. 2022;55:1322-1343.
69. Zhou R, Ji B, Kong Y, et al. PET imaging of neuroinflammation in Alzheimer's disease. *Front Immunol*. 2021;12:739130.

70. Wimberley C, Lavis S, Hillmer A, Hinz R, Turkheimer F, Zanotti-Fregonara P. Kinetic modeling and parameter estimation of TSPO PET imaging in the human brain. *Eur J Nucl Med Mol Imaging*. 2021;49(1):246-256.
71. Narayanaswami V, Dahl K, Bernard-Gauthier V, Josephson L, Cumming P, Vasdev NJ. Emerging PET radiotracers and targets for imaging of neuroinflammation in neurodegenerative diseases: outlook beyond TSPO. *Mol Imaging*. 2018;17:1536012118792317.
72. Walker KA, Ficek BN, Westbrook RJ. Understanding the role of systemic inflammation in Alzheimer's disease. *ACS Chem Neurosci*. 2019;10(8):3340-3342.
73. Xie J, Van Hoecke L, Vandenbroucke RE. The impact of systemic inflammation on Alzheimer's disease pathology. *Front Immunol*. 2022;12:796867.
74. Shepherd CE, Grace EM, Mann DMA, Halliday GM. Relationship between neuronal loss and 'inflammatory plaques' in early onset Alzheimer's disease. *Neuropathol Appl Neurobiol*. 2007;33:328-333.
75. Elahi FM, Casaletto KB, La Joie R, et al. Plasma biomarkers of astrocytic and neuronal dysfunction in early-and late-onset Alzheimer's disease. *Alzheimers Dement*. 2020;16(4):681-695.
76. Arboleda-Velasquez JF, Lopera F, O'Hare M, et al. Resistance to autosomal dominant Alzheimer's disease in an APOE3 Christchurch homozygote: a case report. *Nat Med*. 2019;25:1680-1683.
77. Petersen ME, Zhang F, Schupf N, et al. Proteomic profiles for Alzheimer's disease and mild cognitive impairment among adults with Down syndrome spanning serum and plasma: an Alzheimer's Biomarker Consortium-Down Syndrome (ABC-DS) study. *Alzheimers Dement (Amst)*. 2020;12:e12039.
78. Hamelin L, Lagarde J, Dorothée G, et al. Distinct dynamic profiles of microglial activation are associated with progression of Alzheimer's disease. *Brain*. 2018;141:1855-1870.
79. Budd Haeberlein S, Aisen P, Barkhof F, et al. Two randomized phase 3 studies of aducanumab in early Alzheimer's disease. *J Prev Alzheimers Dis*. 2022;9:197-210.
80. Haddad HW, Malone GW, Comardelle NJ, Degueure AE, Kaye AM, Kaye ADJHPR. Aducanumab, a novel anti-amyloid monoclonal antibody, for the treatment of Alzheimer's disease: a comprehensive review. *Health Psychol Res*. 2022;10:31925.
81. Van Dyck CH, Swanson CJ, Aisen P, Bateman RJ, Chen C, Gee M, et al. Lecanemab in early Alzheimer's disease. *N Engl J Med*. 2023;388:9-21.
82. McDade E, Cummings JL, Dhadda S, et al. Lecanemab in patients with early Alzheimer's disease: detailed results on biomarker, cognitive, and clinical effects from the randomized and open-label extension of the phase 2 proof-of-concept study. *Alzheimers Res Ther*. 2022;14:1-17.
83. Sperling RA, Jack , Black SE, et al. Amyloid-related imaging abnormalities in amyloid-modifying therapeutic trials: recommendations from the Alzheimer's Association Research Roundtable Workgroup. *Alzheimers Dement*. 2011;7:367-385.
84. Charil A, Shcherbinin S, Southeikal S, et al. Tau subtypes of Alzheimer's disease determined in vivo using flortaucipir PET imaging. *J Alzheimers Dis*. 2019;71:1037-1048.
85. Vogel JW, Young AL, Oxtoby NP, et al. Four distinct trajectories of tau deposition identified in Alzheimer's disease. *Nat Med*. 2021;27:871-881.
86. Ferreira D, Nordberg A, Westman E. Biological subtypes of Alzheimer disease: a systematic review and meta-analysis. *Neurology*. 2020;94:436-448.
87. Wheatley S, Mohanty R, Ferreira D, et al. Neurodegenerative pathways in Alzheimer's disease subtypes. *Alzheimer's Dement*. 2022;18:e067749.
88. Ferreira D, Verhagen C, Hernández-Cabrera JA, et al. Distinct subtypes of Alzheimer's disease based on patterns of brain atrophy: longitudinal trajectories and clinical applications. *Sci Rep*. 2017;7:46263.

#### SUPPORTING INFORMATION

Additional supporting information can be found online in the Supporting Information section at the end of this article.

**How to cite this article:** Rossano SM, Johnson AS, Smith A, et al. Microglia measured by TSPO PET are associated with Alzheimer's disease pathology and mediate key steps in a disease progression model. *Alzheimer's Dement*. 2024;1-11. <https://doi.org/10.1002/alz.13699>